A Novel Silk Fiber–Based Scaffold for Regeneration of the Anterior Cruciate Ligament

Histological Results From a Study in Sheep

Andreas Teuschl,*†‡ PhD, Patrick Heimel,†§ MSc, Silvia Nürnberger,‡‖ PhD, Martijn van Griensven,¶ MD, PhD, Heinz Redl,†‡ PhD, and Thomas Nau,†‡# MD
Investigation performed at the Ludwig Boltzmann Institute for Experimental and Clinical Traumatology, AUVA Research Center, Vienna, Austria

Background: Because of ongoing problems with anterior cruciate ligament (ACL) reconstruction, new approaches in the treatment of ACL injuries, particularly strategies based on tissue engineering, have gained increasing research interest. To allow for ACL regeneration, a structured scaffold that provides a mechanical basis, has cells from different sources, and comprises mechanical as well as biological factors is needed. Biological materials, biodegradable polymers, and composite materials are being used and tested as scaffolds. The optimal scaffold for ACL regeneration should be biocompatible and biodegradable to allow tissue ingrowth but also needs to have the right mechanical properties to provide immediate mechanical stability.

Hypotheses: The study hypotheses were that (1) a novel degradable silk fiber–based scaffold with mechanical properties similar to the native ACL will be able to initiate ligament regeneration after ACL resection and reconstruction under in vivo conditions and (2) additional cell seeding of the scaffold with autologous stromal vascular fraction–containing adipose-derived stem cells will increase regenerative activity.

Study Design: Controlled laboratory study.

Methods: A total of 33 mountain sheep underwent ACL resection and randomization to 2 experimental groups: (1) ACL reconstruction with a scaffold alone and (2) ACL reconstruction with a cell-seeded scaffold. Histological evaluation of the intra-articular portion of the reconstructed/regenerated ligament was performed after 6 and 12 months.

Results: After 6 months, connective tissue surrounded the silk scaffold with ingrowth in some areas. The cell-seeded scaffolds had a significant lower silk content compared with the unseeded scaffolds and demonstrated a higher content of newly formed tissue. After 12 months, the density of the silk fibers decreased significantly, and the ingrowth of newly formed tissue increased in both groups. No differences between the 2 groups regarding silk fiber degradation and regenerated tissue were detected at 12 months.

Conclusion: The novel silk fiber–based scaffold was able to stimulate ACL regeneration under in vivo conditions. Additional cell seeding led to increased tissue regeneration and decreased silk fiber content at 6 months, whereas these differences were not present at 12 months.

Clinical Relevance: ACL regeneration using a silk fiber–based scaffold with and without additional cell seeding may provide a new treatment option after joint injuries.

Keywords: autologous stem cells; stromal vascular fraction; tissue engineering; anterior cruciate ligament

Injuries of the anterior cruciate ligament (ACL) result in annual costs of around US$6 billion according to the National Center of Health Statistics.[15] About 350,000 ACL reconstructions are performed in the United States every year (unpublished data: Goodwin E. Presented at the American Orthopaedic Society for Sports Medicine Annual Meeting on Allografts in Orthopaedic Sports Medicine, 2005). Surgical reconstruction has become the method of choice for more than 2 decades, despite the well-documented problems associated with autograft materials, such as anterior knee pain, infrapatellar contracture, muscle weakness, and limited graft availability.[32] Allograft materials, on the other hand, carry the risk for the transmission of bloodborne diseases.[35,40] In young and active patients, ACL

The American Journal of Sports Medicine, Vol. 44, No. 6
DOI: 10.1177/0363546516631954

reconstruction also has a relatively high failure rate, with the consequent need for revision surgery.[24] In addition, the development of posttraumatic osteoarthritis still appears to be an unresolved fact of this surgical strategy.[46]

Because of these ongoing issues with ACL reconstruction, there is a need to develop new approaches that may lead to better outcomes. One such approach is ACL regeneration in which a structured scaffold provides the mechanical basis for initial stability and to regenerate the ligament, together with cells from different sources and biological as well as mechanical modulators. Finding the right biomaterial that may function as a potential scaffold certainly is one of the key challenges. It has to be biocompatible and biodegradable to allow tissue ingrowth, which is crucial for the new ligament to form. Ideally, the scaffold's mechanical properties mimic the natural ACL of any age as close as possible to provide immediate mechanical stability after implantation. Biological materials, biodegradable polymers, and composite materials are under evaluation for ligament engineering.[29,31,35] Among these, silk has been proven to be an attractive candidate.[2,3] Compared with other biomaterials, it has remarkable mechanical strength and toughness. In combination with its slow rate of degradation, it theoretically allows the gradual transfer of stabilizing properties from the graft to the newly forming tissue without exposing the patient to periods of joint laxity.

The slow degradation of silk is based on its biological inertness.[1,10] In contrast to grafts fabricated of other biomaterials such as collagen, there is no special enzyme produced by cells[41] that can lead to an unwanted fast reduction of mechanical properties. Silk, like other proteins, is degraded to peptides that are metabolized by cells and do not lead to an immunological response, as has been reported with the degradation of synthetic polymers, for example.[5]

Silk fibers have been used as a raw material for ACL scaffolds, and it has been demonstrated that the twisted fiber scaffolds are able to match the mechanical properties of the native human ACL.[2,17] In previous studies, an ACL graft based on silk fibers in a wire rope design[16] and a method to efficiently remove the immune-eliciting sericin from high hierarchical textile-engineered matrices based on raw silk fibers[44] have been developed. The possibility of removing sericin well after the textile-engineering process eases the production of highly ordered scaffold structures by making use of the sliding properties of the sericin surface proteins. The resulting sericin-free silk ACL grafts show ultimate tensile strength and elasticity values (Figure 1C), comparable with native ovine ACL tissue.[8,19,27,33,47]

The first aim of the present study was to determine if this novel degradable silk fiber–based scaffold is able to initiate ACL regeneration under in vivo conditions. Our second aim was to determine if there is a difference in ACL regeneration between a cell-seeded scaffold (CS) and the implantation of the silk fiber–based scaffold alone (SA). We hypothesized that a novel degradable silk fiber–based scaffold would be able to initiate ligament regeneration after ACL transection and reconstruction. We also hypothesized that additional cell seeding of the scaffold with autologous stromal vascular fraction–containing adipose-derived stem cells[6,22,23] would lead to increased regenerative activity.

METHODS

If not indicated otherwise, all reagents were purchased from Sigma and were of analytical grade. The study design was approved by the local ethical committee.

Study Design

A total of 33 female mature mountain sheep with a mean (±SD) body weight of 64.4 ± 3.7 kg were selected and randomized to 1 of 2 experimental groups: (1) ACL regeneration with an SA and (2) ACL regeneration with a CS. Half of the sheep within each group were followed up to 6 months (n = 8 each for SA and CS) and half to 12 months (n = 8 for SA, n = 9 for CS).

Preparation of the Silk Fiber–Based Scaffold Device

The silk fiber–based scaffolds were fabricated as previously described.[16,44] Briefly, white raw *Bombyx mori* silkworm fibers of 20/22 den and 250 T/m (Testex AG) were braided into wire rope–like structures in cooperation with Edelrid, consisting of a core and a sheathing element (Figure 1, A and B). The inner core component was formed by 2 strands, which were enveloped by a tubular sheathing structure. The entire scaffold has a total diameter of 4 mm.

To remove the possible antigenic-eliciting sericin proteins, the silk scaffolds were boiled in borate buffer as previously described.[44] The samples were then thoroughly washed in ddH_2O, dried in a heating cabinet (T6060; Heraeus) at 100°C for approximately 3 hours, and individually packaged and sterilized by steam autoclaving (Melatronic 23; Melag Medizintechnik) at 121°C.

The prepared silk fiber–based scaffold devices were then mechanically tested via tension-to-failure testing as described by Hohlrieder et al.[16] Briefly, scaffolds were immersed in phosphate-buffered saline (PBS) for at least

[#]Address correspondence to Thomas Nau, MD, Ludwig Boltzmann Institute for Experimental and Clinical Traumatology, AUVA Research Center, Koschatgasse 2/6, Vienna 1190, Austria (email: thnau@hotmail.com).
[*]Department of Biochemical Engineering, University of Applied Sciences Technikum Wien, Vienna, Austria.
[†]Ludwig Boltzmann Institute for Experimental and Clinical Traumatology, AUVA Research Center, Vienna, Austria.
[‡]Austrian Cluster for Tissue Regeneration, Vienna, Austria.
[§]Karl Donath Laboratory for Hard Tissue and Biomaterial Research, Medical University of Vienna, Vienna, Austria.
[‖]Department of Traumatology, Medical University of Vienna, Vienna, Austria.
[¶]Department of Experimental Trauma Surgery, Technical University of Munich, Munich, Germany.
One or more of the authors has declared the following potential conflict of interest or source of funding: A.T. and H.R. have applied for a patent for a new technique of sericin removal (PCT/EP2013/070213).

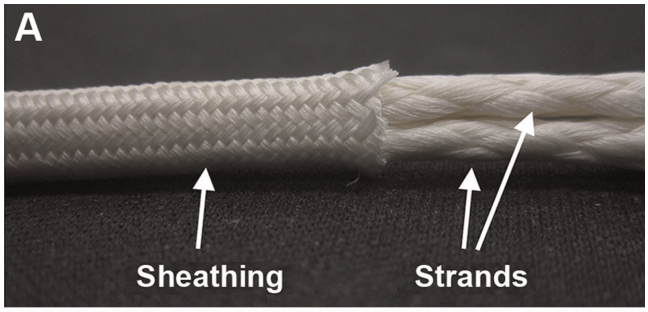

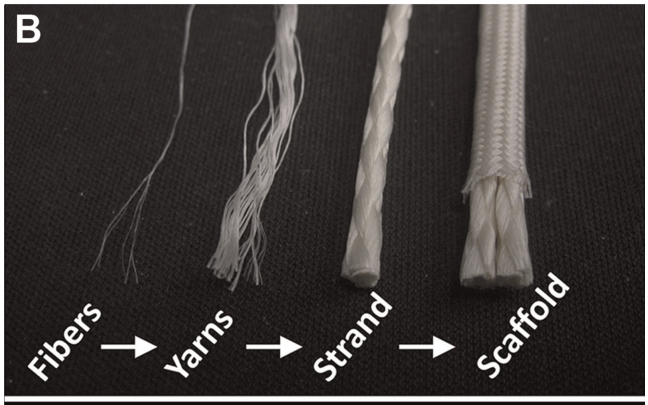

C	Ultimate tensile strength, N	Stiffness, N/mm
Silk-based graft (current study)	1450 ± 65	194 ± 27
Literature data		
Hunt et al[19]	1513 ± 180	143.9 ± 16.1
Dustmann et al[8]	1670.5 ± 375.6	173.0 ± 19.6
Mayr et al[33]	1764.0 ± 361.9	259.6 ± 62.0
Weiler et al[47]	1531 ± 180	
Laitinen et al[27]	1425 ± 712	

Figure 1. Description of the silk fiber–based anterior cruciate ligament (ACL) graft. (A) Gross observation showing the wire rope design of the silk scaffold, consisting of 2 strands forming the inner core enveloped by tubular sheathing. Notable are the individual braiding designs of the core and sheathing elements that are visible. (B) The silk ACL scaffold is based on single *Bombyx mori* silk fibers. These fibers are assembled into yarns and textile engineered into higher hierarchical structure strands or sheathing forming the entire scaffold. (C) Mechanical properties of the silk-based scaffold (ultimate tensile strength and stiffness values) compared with native ACL structures (values from other studies). n = 10.

1 hour before testing. Stress-strain curves were recorded using a materials testing machine (Z050; Zwick GmbH & Co KG) at a strain rate of 5 mm/min with 100 N of pretension to determine ultimate tensile strength; the linear portion of the stress-strain curve was used to calculate stiffness values. The silk fiber–based scaffolds showed values of 1450 ± 65 N for ultimate tensile strength and 194 ± 27 N/mm for stiffness (Figure 1C), which were in the range of reported mechanical values for an intact sheep ACL.[8,19,27,33,47]

Surgical Technique

A medial arthrotomy was performed, and the fat pad was partially resected (Figure 2, A-C). The exposed ACL was removed by transecting the ligament close to its femoral and tibial origins. The resected fat pad was further used for preparing a stromal vascular fraction in the CS group (Figure 2, H-J).

ACL Reconstruction With the Silk Fiber–Based Scaffold. After ACL removal, the knees were prepared similarly as in conventional ACL reconstruction. A 4.0-mm tunnel was drilled through the proximal tibia, exiting the tibial surface exactly in the center of the tibial ACL footprint (Figure 2D). Another 4.0-mm tunnel was drilled through the lateral femoral condyle, addressing the femoral ACL footprint in the same way. The silk fiber scaffold (6 cm in length and 4 mm in diameter) was armed with nonabsorbable sutures (Mersilene 1; Johnson & Johnson) on either end using a whipstitch technique (Figure 2E). After the edges of the tunnels were smoothed, the scaffold was pulled through the knee (Figure 2F) and adjusted for central placement, leaving 1.5 to 2.0 cm on either side in the bony tunnels. Cortical scaffold fixation was achieved with custom-made fixation buttons proximally and distally (Figure 2G). After femoral fixation, the scaffold was firmly tensioned with the knee in maximal extension, followed by tibial cortical fixation.

For the animals in the CS group, the same ACL reconstruction procedure was performed. Parallel to the surgical procedure, the previously harvested fat pad was used to prepare the stromal vascular fraction (Figure 2, H-J) as previously described.[7,23] Briefly, the explanted knee fat pad was washed thoroughly with PBS and minced into small pieces of 5 to 20 mm^3. These explants were then incubated with collagenase type 1 (Biochrome) at 37°C for 45 minutes in a 50-mL Falcon tube under constant rotation at 10 rpm via a rotator (PTR-35; Grant Instruments). After centrifugation at 600*g* for 5 minutes, the stromal vascular fraction was collected suspended in 50 μL Dulbecco's modified Eagle's medium (DMEM)/Ham's F12 without supplements and mixed with 50 μL of the fibrinogen component (100 mg/mL fibrinogen) of the fibrin sealant Tisseel (Baxter AG). Prior to this step, the fibrinogen (final concentration of 100 mg/mL) and thrombin components (final concentration of 4 IU/mL) were reconstituted with 40 mM $CaCl_2$ and with a 3000 U/mL aprotinin solution at 37°C, respectively. Syringes were filled with the cell-loaded fibrinogen component and the thrombin component of the sealant and were mounted for application in a Duploject syringe holder (Baxter AG).

After ACL reconstruction (Figure 2K), the cell–fibrin glue suspension was meticulously injected under the superficial layer of the scaffold within the entire intra-articular portion as well as within the bony tunnels (Figure 2J). All incisions were closed in layers. After surgery, the

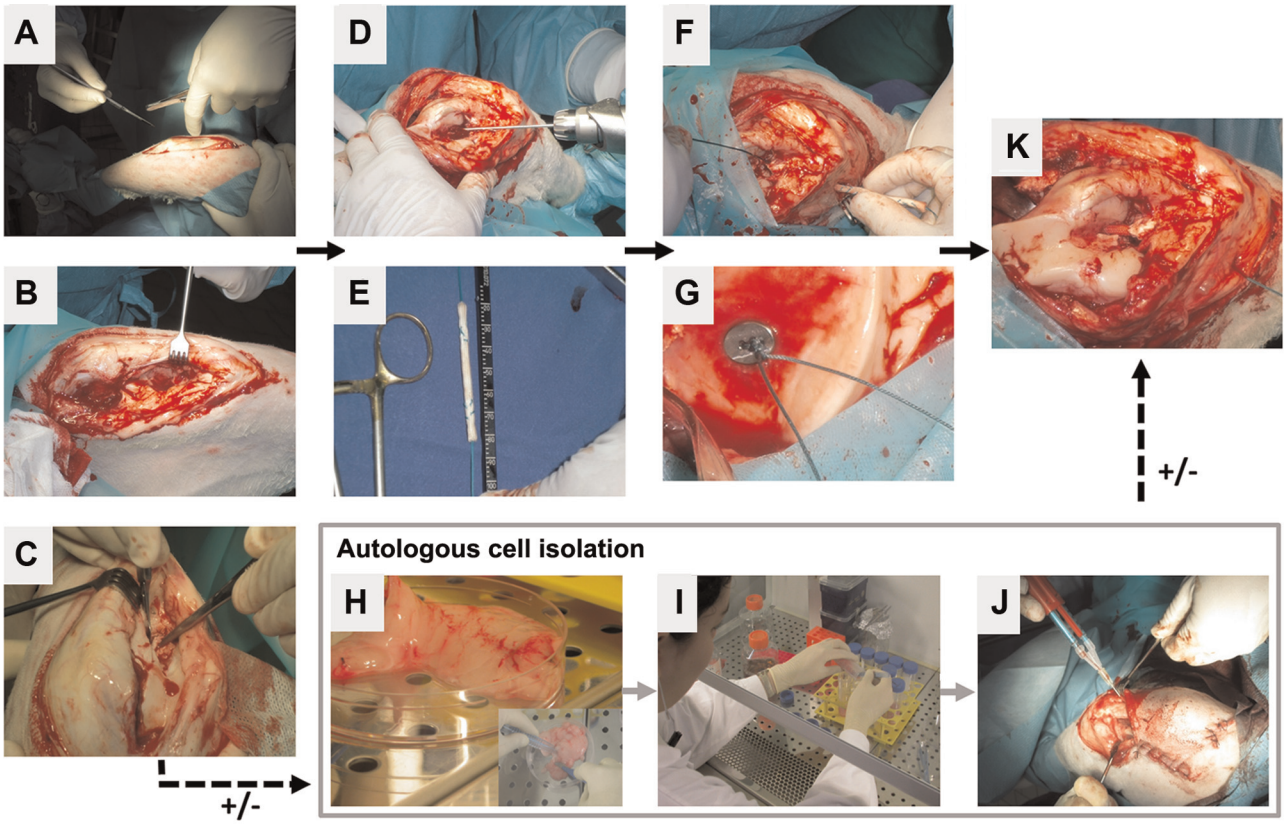

Figure 2. Surgical procedure. (A, B) After arthrotomy and anterior cruciate ligament (ACL) resection, anatomic ACL reconstruction is performed, exactly addressing the anatomic footprints of the natural ACL. (C) The infrapatellar fat pad is resected for optional autologous stromal vascular fraction isolation (gray box). (D) After drilling of bone tunnels, (E) the 6 cm–long scaffold is armed with nonabsorbable sutures similar to a tendon graft, (F) the scaffold is pulled through the knee joint in the course of the natural ACL, and (G) cortical fixation is administered with custom-made fixation buttons. (H, I) Stromal vascular fraction isolation is performed in parallel to the surgical procedure, and the isolated autologous cell mixture is suspended in fibrin glue and injected into the scaffold after the reconstructive procedure in the cell-seeded group. (J) Intra-articular view of (K) completed ACL reconstruction.

animals were housed for 6 weeks in separated pens of 3 sheep each and were then allowed to join the herd on the farm. After 6 and 12 months, the animals were euthanized, and the limbs were harvested and immediately put into neutral buffered 10% formalin for up to 48 hours. Then, the samples were thoroughly rinsed with tap water and stored in 70% ethanol until further workup.

Macroscopic Assessment

After tissue harvest, the knee joints were macroscopically assessed for ligament integrity and for any degenerative changes in all compartments by the senior surgeon (T.N.), who was blinded to the treatment group.

Ligament Histology

The microscopic evaluation was performed by 2 authors (A.T., P.H.), who were blinded to the treatment group and the time point. For the histological workup, the intra-articular portion of the ACL was removed in total from the specimen and further dehydrated with an increase in graded series of alcohol and embedded in paraffin via the intermedium xylol. Samples were sectioned 3 to 4 μm thick using a rotatory microtome (HM 355S Microm; Thermo Fisher Scientific Inc), deparaffinized, and rehydrated in a graded series of alcohol. Sections of all samples were stained for martius scarlet blue (MSB) staining. MSB staining comprises several labeling steps containing martius yellow, brilliant crystal scarlet, and phosphotungstic acid and stains blue for collagen, red/orange for silk, violet for nuclei, and yellow for erythrocytes. In addition, hematoxylin and eosin staining was performed to analyze the cell phenotype in terms of nuclearity (mononuclear vs polynuclear). To demonstrate the formation of aligned collagen fibers along the silk fibers of the graft, the mechanical load sections were stained with picrosirius red and imaged with circularly polarized light microscopy (E800; Nikon GmbH).

Segmentation

The images were loaded into Developer XD 2.1 (Definiens AG). After downsampling the images to a resolution of 0.642 μm/pixel, multiresolution segmentation was performed as described elsewhere.[4] Violet, blue, yellow, and red tissues were classified based on relations between the different color layers as well as relationships between neighboring objects. As silk fibers appear mostly as round and oval objects, erosion and dilation steps were applied to obtain improved quantification.

The resulting classification was exported, and the position of the longitudinal and cross-sectional cuts was marked using Photoshop CS5 (Adobe Systems). Damaged sections of the cross-section were always excluded in the shape of a wedge from the center of the scaffold all the way to the edge of the cross-section. Of the longitudinal cuts, only areas where the entire width of the sample was intact were included for the measurements.

The marked images were then imported into Definiens Developer XD 2.1. The classification was restored and the regions marked in Photoshop detected. On some sections, parts of the sample were missing in the center of the section. These missing areas were always surrounded by silk, which was poorly infiltrated by tissue. To allow these sections to be measured, these regions were assigned a relative area based on the surrounding classes using the following process. The missing regions were separated in 82 μm–wide squares, and the percentage area of the different classes within 657 μm of each object at the edge of the missing region was measured. The square objects inside the missing region were processed from the edge of the region toward the center by measuring (1) the average of the area's percentage previously measured for objects at the edge of the missing region and the percentages determined for other objects in previous iterations of this process within 328 μm and (2) the area of violet, blue, yellow, and red tissues as well as the partitions of the missing regions. An additional analysis was performed measuring the same parameters while excluding the sheath of predominately blue tissue surrounding the silk scaffold.

Statistical Analysis

All calculations were performed using GraphPad software (GraphPad Software Inc). All data are presented as mean ± SD. The normal distribution of data was tested with the Kolmogorov-Smirnov test. An analysis of variance was used to conduct multiple pairwise comparisons between the different groups, followed by the Bonferroni test for post hoc analysis. In addition, linear regression analysis was performed to identify the influence of the degrading silk content on the newly regenerated tissue and on the cellularity of the constructs. Statistical significance was set at $P < .05$.

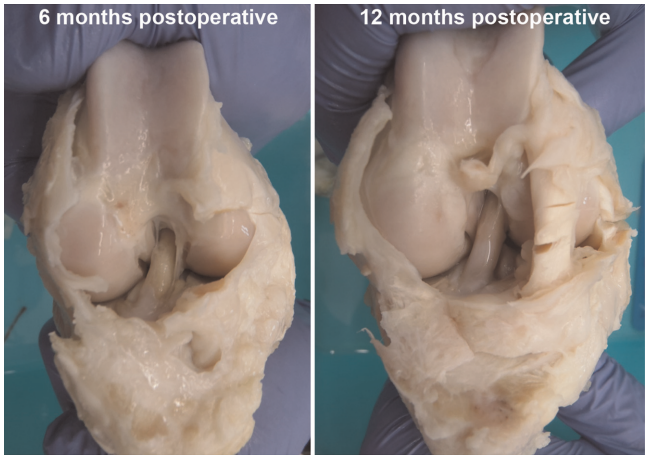

Figure 3. Macroscopic view of anterior cruciate ligament (ACL) reconstruction after 6 and 12 months. The regenerated ACLs all appeared as strong ligament-like structures in the course of the natural ACL.

RESULTS

Animal Welfare

One animal died of tympanites, and another animal had to be sacrificed 2 weeks postoperatively because of a joint infection; both animals were from the 6-month SA group. All other animals achieved unrestricted full weightbearing within 24 hours. Wound healing in these 31 sheep was uneventful, and no further joint-related clinical problems were found. At 6 months, the total number of animals was 6 in the SA group and 9 in the CS group. At 12 months, the total number of animals was 8 in the SA group and 8 in the CS group.

Macroscopic Assessment

There were no macroscopic signs of cartilage degeneration or lesions in any animals in the 2 experimental groups after 6 and 12 months. The regenerated ACLs all appeared as strong ligament-like structures (Figure 3) in the course of the natural ACL in both groups and at both time points. There were no ruptures or any other form of macroscopic ligament lesions evident.

Ligament Histology

Six months after surgery, the silk fibers of the scaffold dominated the histological picture (Figure 4, A and B). The cross-sections demonstrated connective tissue surrounding the silk fibers. Ingrowth of the connective tissue between the fibers was seen in some areas.

The histological segmentation of the entire construct after 6 months (Figure 5, A1) did show significant differences in the relative silk content ($P = .0226$) as well as

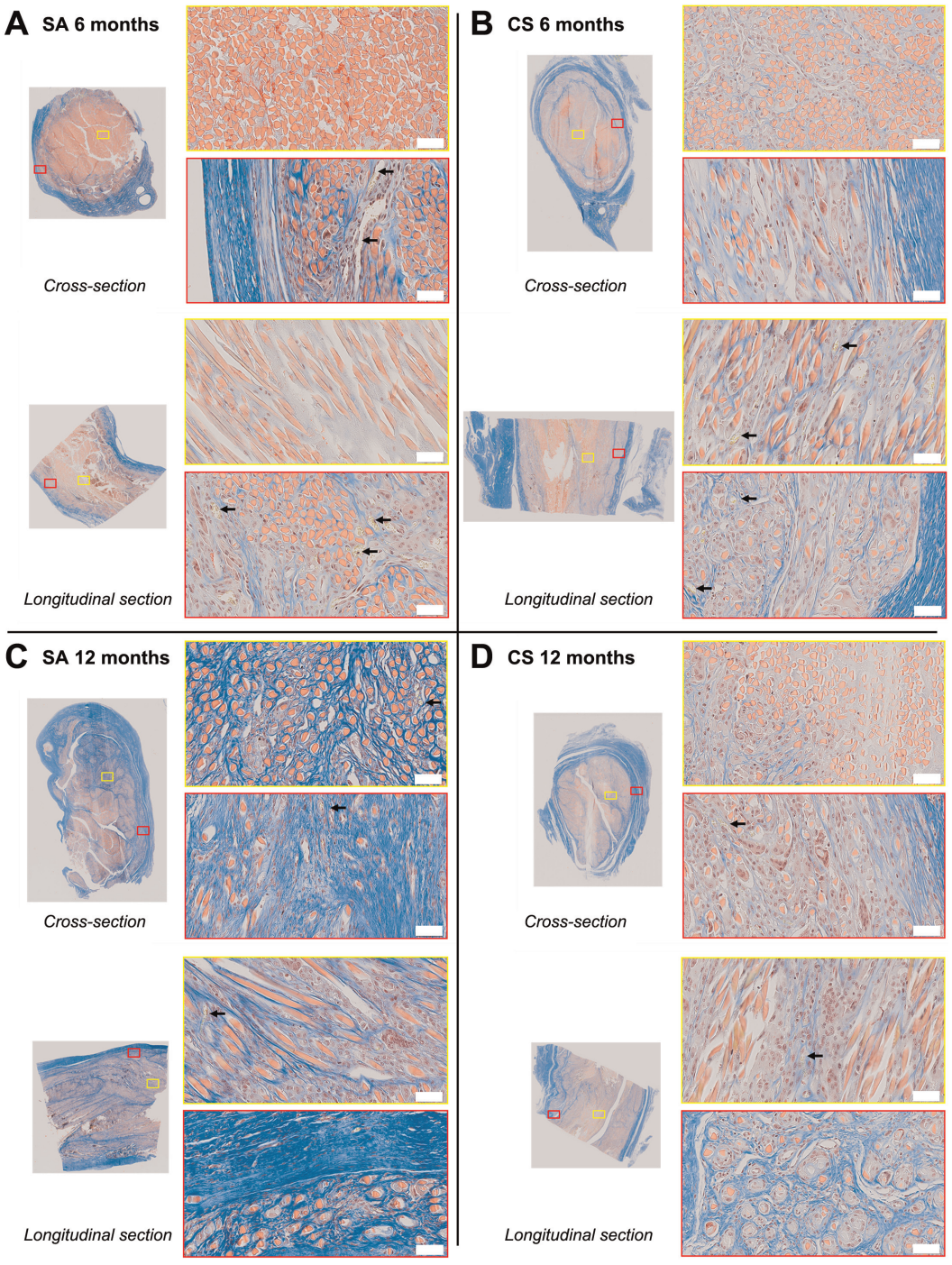

Figure 4. Histology staining, martius scarlet blue: Overview of the histological picture comparing the 2 experimental groups (scaffold alone [SA] vs cell-seeded scaffold [CS]) and the 2 time points (6 vs 12 months). (A, B) After 6 months, connective tissue is surrounding the silk fiber–based grafts with ingrowth in some areas. In the CS group, a higher cell content in the inner parts of the structure is observable. (C, D) After 12 months, tissue ingrowth increases, and silk fiber degradation is obvious. In terms of tissue growth and silk fiber reduction, no differences between the 2 groups were seen anymore. Arrows indicate observed blood vessel formation inside the scaffolds. Scale bar = 50 μm.

relative tissue content ($P < .0170$) between the SA and CS groups. The cell-loaded scaffolds showed a lower relative content of silk compared with plain scaffolds (16.77% ± 9.87% vs 31.66% ± 13.41%, respectively), combined with a higher content of newly formed tissue after 6 months (66.59% ± 10.11% vs 49.19% ± 14.10%, respectively). From 6 to 12 months, the mean values of the SA group for the relative silk content decreased from 31.66% ±

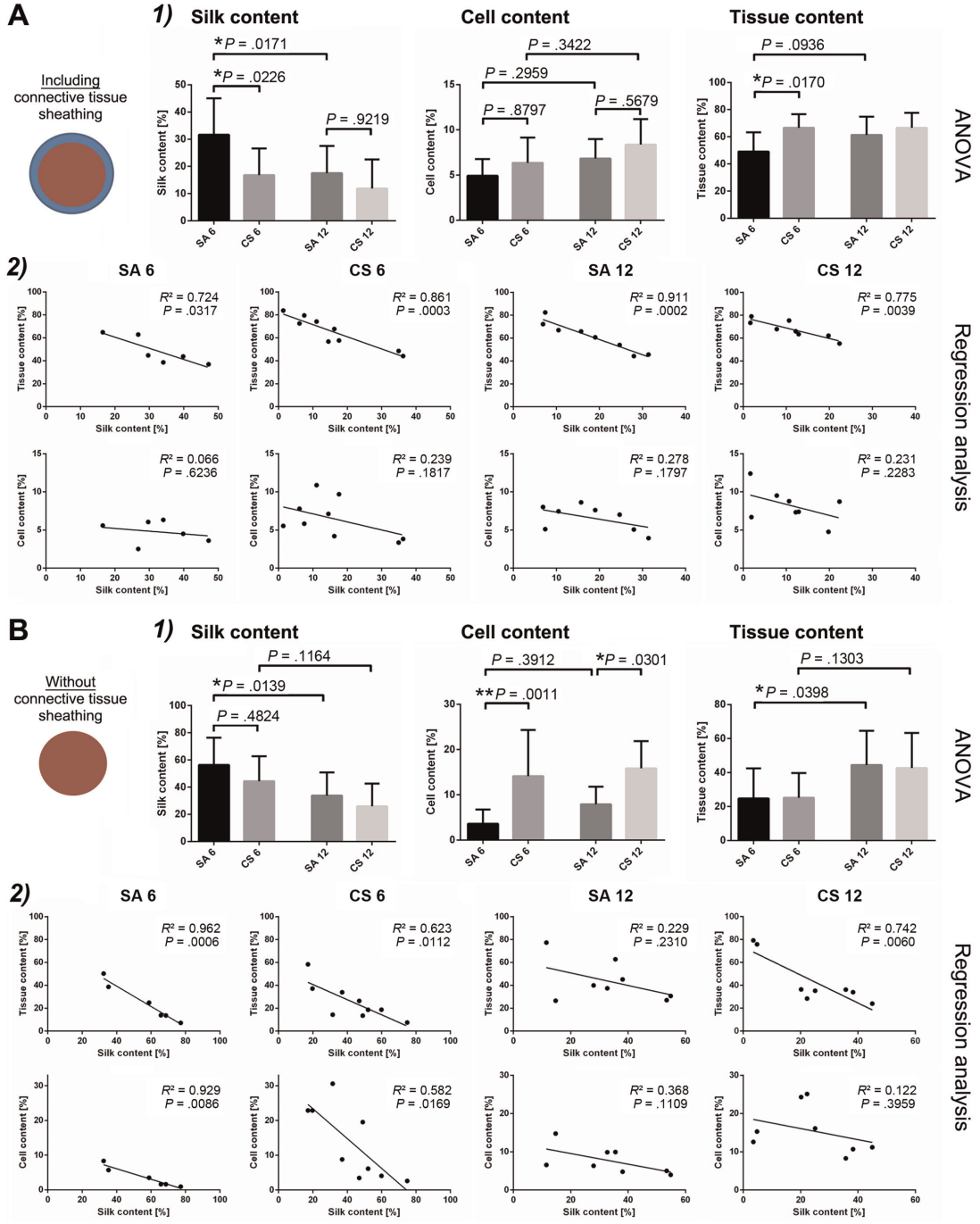

Figure 5. Quantitative determination of silk, cell, and tissue content of the regenerated anterior cruciate ligament structures in (A) the whole graft structure, including connective tissue sheathing, and in (B) the silk graft structure alone, respectively. In each bar graph, the 2 experimental groups (scaffold alone [SA] vs cell-seeded scaffold [CS]) and the 2 time points (6 vs 12 months) are compared. Remarkably, the cell content in the CS group was higher after 6 and 12 months when evaluating only the inner structure. Regarding the whole construct, the CS group showed a decreased silk content in combination with a higher regenerated tissue content. After 12 months, no differences in terms of degenerated silk content and regenerated tissue content were detectable. n $\geq$ 6 animals, mean $\pm$ SD. All *P* values not added in the figure are higher than .90. Statistically significant difference: *$P <$ .05, **$P <$ .01. (A2, B2) Linear regression analysis of the cell content and formed tissue against the residual silk content, including the respective R^2 and *P* values. Overall, a negative correlation between the newly formed tissue and the silk content was found, which was significant throughout all groups and time points with only 1 exception (12-month SA group in B2). A negative correlation between the cellularity of the grafts and silk content could also be seen but was only significant in the 6-month SA group, evaluating the graft without connective tissue sheathing.

13.41% to 17.53% ± 10.03%, whereas the tissue content and relative cell content increased from 49.19% ± 14.10% to 61.33% ± 13.51% (P = .0936) and from 4.91% ± 1.85% to 6.82% ± 2.15% (P = .2959), respectively. As a consequence, statistical differences were no longer detectable between the SA and CS groups after 12 months in terms of reduced silk content and increased cell content as well as newly formed tissue content (Figure 5A, upper panel).

By looking only at the inner part of the construct, the segmentation results demonstrated a significantly higher relative cell content (P = .0011) in the CS group (14.12% ± 10.20%) compared with the SA group (3.60% ± 3.13%) after 6 months (Figure 5, B1), whereas the other parameters did not reveal any significant differences. The mean value of the relative silk content in the CS group after 6 months (44.36% ± 18.37%) was lower (P = .4824) than that in the SA group (56.37% ± 20.02%). For the 6-month time point, the mean values for the relative content of newly formed tissue for both groups were comparable (24.79% ± 17.65% and 25.19% ± 14.59% for the SA and CS groups, respectively).

Similar to the analysis of the entire construct, the inner part showed decreasing silk content and increased tissue content from 6 to 12 months in both the SA and CS groups (Figure 5, B1). The relative silk content decreased significantly (P = .0139) from 56.37% ± 20.02% to 33.83% ± 17.08% in the SA group and from 44.36% ± 18.37% to 25.90% ± 16.70% in the CS group (P = .1164). Conversely with the decreasing relative silk content, the relative tissue content increased significantly (P = .0398) from 24.79% ± 17.65% to 44.46% ± 20.13% for the SA group and from 25.19% ± 14.59% to 42.63% ± 20.69% for the CS group (P = .1303).

Despite an increase in the relative cell content of the SA grafts from 3.60% ± 3.13% to 7.88% ± 9.32% (P = .3912) over the time period, cellularity was still significantly lower than that in the CS group (15.84% ± 5.99%) after 12 months regarding only the inner part of the construct (P = .0301).

Based on linear regression models, the magnitude of silk degradation correlated with newly formed tissue but not with cellularity of the ligament grafts. In general, the more the silk content decreased, the more tissue was formed (Figure 5). The relationship between silk content and tissue formation was significant throughout all time points (at 6 months: R^2 = 0.724, P = .0317 [SA] and R^2 = 0.861, P = .0003 [CS]; at 12 months: R^2 = 0.911, P = .0002 [SA] and R^2 = 0.775, P = .0039 [CS]) evaluating the whole graft. By evaluating only the tissue formation without the formed connective tissue sheathing, the relationship was significant for the SA group at 6 months (R^2 = 0.962, P = .0006) and the CS group at 12 months (R^2 = 0.742, P = .0060;) but not for the CS group at 6 months (R^2 = 0.623, P = .0112) or the SA group at 12 months (R^2 = 0.229, P = .2310).

No statistically significant correlation between cell content and silk content was detectable by regression analysis throughout all treatment groups and time points (detailed R^2 and P values can be found in Figure 5) with the exception of the 6-month SA group (R^2 = 0.929, P = .0086).

Collagen Deposition and Cell Phenotype

The vast majority of cells in the silk grafts after 6 and 12 months were mononuclear (Figure 6), and only a sparse amount of polynuclear foreign-body giant cells were visible. No difference in terms of the phenotype between the cells in the SA and CS groups as well as between time points could be observed. Moreover, erythrocytes could be seen in some areas, indicating blood vessel formation in the developing tissue. The mononuclear cells were in close relation with the newly formed tissue, which consisted mainly of collagenous tissue, as indicated by performed picrosirius red staining (Figure 7, A and B). The deposited collagen fibers showed an orientation along the braiding design of the silk fibers (Figure 7C).

DISCUSSION

The results of this study support the first hypothesis that the novel silk fiber–based scaffold initiated regeneration of the ligament. The changing histological picture from the 6-month to the 12-month time points clearly demonstrated the regenerative process (Figure 4, A-D). In parallel to the increase of regenerated tissue, a degradation of silk fibers took place. Despite these findings, the amount of silk fibers after 12 months was actually larger than expected.

The results partially supported the second hypothesis that cell seeding of the scaffold with autologous stromal vascular fraction–containing adipose-derived stem cells results in increased regenerative capacity. Cell seeding led to increased regeneration within the first 6 months for the entire construct (Figure 5A, upper panel). Interestingly, after 12 months, the SA group caught up in terms of regenerated tissue, and no significant difference between the 2 groups was seen anymore. In addition, cell seeding seems to have had an effect on the degradation of silk fibers. The increased regenerated tissue in the CS group after 6 months went hand in hand with a reduction of silk fibers compared with the SA group (Figure 5, A and B [correlation analysis]). Again, after 12 months, this difference was not detected anymore.

The option of using a tissue-engineered ACL to overcome the problems of the current standard reconstruction techniques was mentioned by several authors.[14,39,45] In a questionnaire by Rathbone et al,[39] 300 surgeons were asked if they would be open to using a tissue-engineered ACL in their patients. For 86%, this was an option provided that the construct provides biological and mechanical success, and for 76% of the participants, a tissue-engineered ACL was superior to any of the autograft reconstruction techniques. It was also mentioned that a fully load-bearing construct is needed and that several ACL regeneration strategies have to address this need for mechanical integrity. We think that this immediate mechanical stability is of crucial importance for any tissue-engineered construct to be able to be translated into clinical practice as the current ACL reconstruction techniques all provide an immediate load-bearing

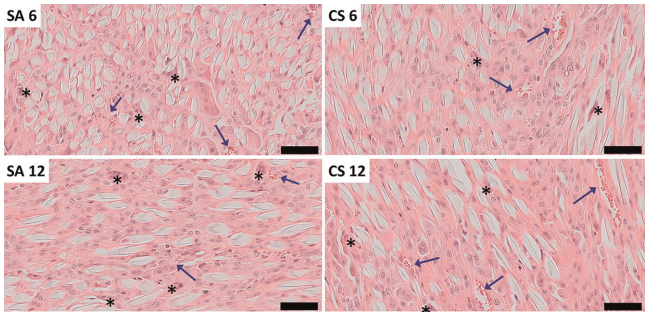

Figure 6. Representative hematoxylin and eosin (H&E)–stained cell-infiltrated silk fiber–based anterior cruciate ligament grafts. Longitudinal sections stained with H&E show the cells surrounding the fibers in the 2 experimental groups (scaffold alone [SA] vs cell-seeded scaffold [CS]) and the 2 time points (6 vs 12 months). The majority of cells are mononuclear. Only a sparse amount of polynuclear cells (asterisks), most likely indicating foreign-body giant cells, are observable. Moreover, blood vessels are present in some areas (arrows). Scale bar = 50 μm.

environment. Many of the different biomaterials used in ligament regeneration lack mechanical stability, despite encouraging biological results.[35]

Silk, on the other hand, is a biomaterial of remarkable strength and toughness and thus an attractive candidate for ACL regeneration.[2,3,11,18,36] Fan et al[9,10] demonstrated promising results using silk ACL grafts in in vivo studies. In both studies, their scaffold was based on a knitted silk mesh, which was rolled up along a silk sponge in a small animal model (rabbit). To meet the required increased mechanical properties of the large animal model (pig), the sponges were replaced by a braided silk cord.[9] In view of clinical translation, this step is in accordance with our scaffold design to use textile-engineering technologies to generate highly mechanically stable grafts.[3] First clinical trials are currently being conducted of silk-based textile-engineered ACL grafts.[42]

The sheep model certainly has the common limitations that all animal models of ACL surgery have. Human conditions are never fully represented in a quadruped, and postoperative rehabilitation is difficult to control in any animal model.[34] We chose the sheep model because sheep are in general very active animals,[13,38] and we wanted to test in vivo ligament regeneration under physiological conditions with early weightbearing and unrestricted range of motion postoperatively. Another limitation of our study may be the short follow-up of only 12 months. Initially, we expected the degradation of silk fibers to be completed after that time. Despite the encouraging results in terms of regenerated ligament tissue, obviously a longer observation period is needed to observe when scaffold degradation is completed. Furthermore, we did not include the bony integration of the construct in the present analysis. This is certainly another crucial aspect of a successful tissue-engineered ACL construct that needs to be considered, especially in the context of eventual translation into clinical practice.

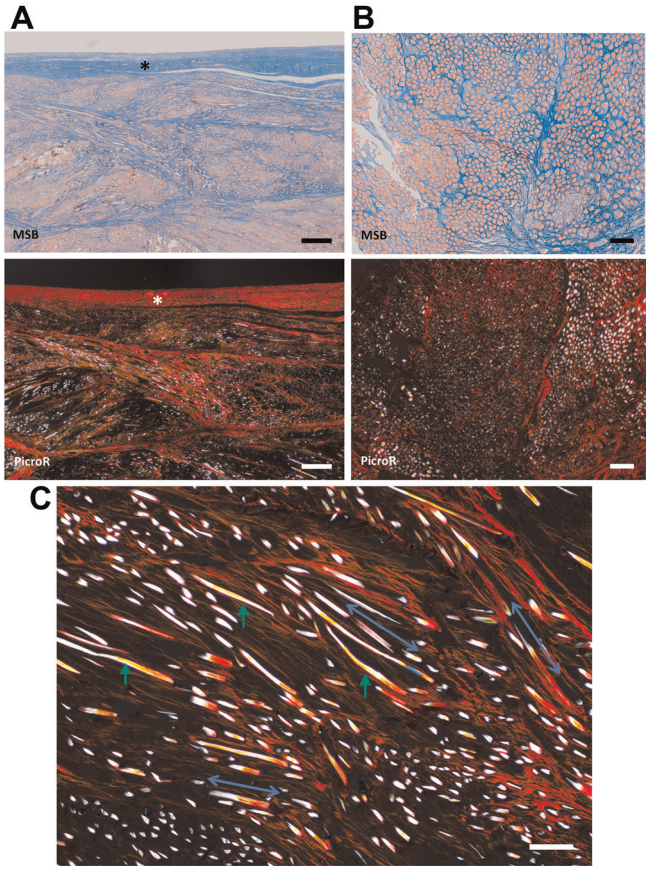

Figure 7. Representative martius scarlet blue (MSB) and picrosirius red (PicroR) staining of the regenerated anterior cruciate ligament (ACL) construct after 12 months, indicating collagen fiber deposition. (A) Longitudinal sections and (B) transverse sections showing the overall distribution and orientation of collagen fibers (stained in red) formed in the ACL scaffold based on silk fibers (appearing in white). (A) The outer layer of collagen fibers on the silk matrix is indicated with asterisks. A longitudinal alignment of the collagen fibers is visible in the inner regions. Scale bar = 500 μm. (B) Newly formed collagen can be seen between the silk fibers. Scale bar = 100 μm. (C) Collagen fibers are aligned in the directions (blue arrows) of the adjacent braided silk fibroin fibers (green arrows). Scale bar = 100 μm.

In this large animal study, we demonstrated that a novel silk fiber–based scaffold was able to initiate ACL regeneration under in vivo conditions, with immediate full weightbearing and without immobilization. Within the first 6 months, additional cell seeding led to increased tissue regeneration and silk fiber degradation. These results are in accordance with those of previous studies in which autologous or degradable ACL grafts[9,10,12,20,30] have been combined with mesenchymal stem cells. However, after 12 months, this effect was not detected anymore, with similar tissue regeneration in both groups, whereas silk fiber degradation was not completed. This is an interesting

finding as it would indicate that the silk graft is infiltrated and remodeled by cells on its own and that there is no need for an additional application of stem cells. The knee joint comprises various cell sources such as residual ruptured ligament tissue or synovium tissue. Cells have been proven to be recruited from these origins and to participate in ligamentous regeneration processes.[21,25,26] In addition, we speculate that the recruitment of regenerating cells is augmented by the drilling of bone holes, giving access to the vasculature of bone tissue similarly to cartilage regeneration studies (eg, microfracturing).[43]

The infiltrated cells in the silk-based graft show predominantly a mononuclear phenotype (Figure 6) and are in close relation to newly formed tissue (Figure 7, A and B). We therefore suggest that these cells are fibroblastic cells depositing the collagenous fibers that are observable using picrosirius red staining. Interestingly, these fibers are oriented along the silk fibers and therefore along the direction of mechanical strain (Figure 7C). This observation is in accordance with other studies showing the deposition of the extracellular matrix along fiber-based grafts.[9,28,37]

We conclude that the observed infiltration by regenerative cells from the surrounding tissues highlights the possibility to generate an off-the-shelf standardized product without the need for additional cells to regenerate the ACL. Despite these encouraging results, further work is needed to address the osteointegration of the construct as well as the overall mechanical performance after complete silk fiber degradation.

REFERENCES

1. Altman GH, Diaz F, Jakuba C, et al. Silk-based biomaterials. *Biomaterials*. 2003;24(3):401-416.
2. Altman GH, Horan RL, Lu HH, et al. Silk matrix for tissue engineered anterior cruciate ligaments. *Biomaterials*. 2002;23(20): 4131-4141.
3. Altman GH, Horan RL, Weitzel P, et al. Clinical, mechanical and histopathological evaluation of a bioengineered long-term bioresorbable silk fibroin graft in a one year goat study for development of functional autologous anterior cruciate ligament. *J Bone Joint Surg Br*. 2012;94(Suppl IV):25.
4. Benz UC, Hofmann P, Willhauck G, Lingenfelder I, Heynen M. Multi-resolution, object-oriented fuzzy analysis of remote sensing data for GIS-ready information. *ISPRS J Photogramm Remote Sens*. 2004;58(3-4):239-258.
5. Cao Y, Wang B. Biodegradation of silk biomaterials. *Int J Mol Sci*. 2009;10(4):1514-1524.
6. Casteilla L, Planat-Benard V, Laharrague P, Cousin B. Adipose-derived stromal cells: their identity and uses in clinical trials, an update. *World J Stem Cells*. 2011;3(4):25-33.
7. Dragoo JL, Samimi B, Zhu M, et al. Tissue-engineered cartilage and bone using stem cells from human infrapatellar fat pads. *J Bone Joint Surg Br*. 2003;85(5):740-747.
8. Dustmann M, Schmidt T, Gangey I, Unterhauser FN, Weiler A, Scheffler SU. The extracellular remodeling of free-soft-tissue autografts and allografts for reconstruction of the anterior cruciate ligament: a comparison study in a sheep model. *Knee Surg Sports Traumatol Arthrosc*. 2008;16(4):360-369.
9. Fan H, Liu H, Toh SL, Goh JCH. Anterior cruciate ligament regeneration using mesenchymal stem cells and silk scaffold in large animal model. *Biomaterials*. 2009;30(28):4967-4977.
10. Fan H, Liu H, Wong EJW, Toh SL, Goh JCH. In vivo study of anterior cruciate ligament regeneration using mesenchymal stem cells and silk scaffold. *Biomaterials*. 2008;29(23):3324-3337.
11. Farè S, Torricelli P, Giavaresi G, et al. In vitro study on silk fibroin textile structure for anterior cruciate ligament regeneration. *Mater Sci Eng C Mater Biol Appl*. 2013;33(7):3601-3608.
12. Figueroa D, Espinosa M, Calvo R, et al. Anterior cruciate ligament regeneration using mesenchymal stem cells and collagen type I scaffold in a rabbit model. *Knee Surg Sports Traumatol Arthrosc*. 2014;22(5):1196-1202.
13. Gregory MH, Capito N, Kuroki K, Stoker AM, Cook JL, Sherman SL. A review of translational animal models for knee osteoarthritis. *Arthritis*. 2012;2012:764621.
14. Hairfield-Stein M, England C, Paek HJ, et al. Development of self-assembled, tissue-engineered ligament from bone marrow stromal cells. *Tissue Eng*. 2007;13(4):703-710.
15. Hing E, Cherry DK, Woodwell DA. National Ambulatory Medical Care Survey: 2004 summary. *Adv Data*. 2006;(374):1-33.
16. Hohlrieder M, Teuschl AH, Cicha K, van Griensven M, Redl H, Stampfl J. Bioreactor and scaffold design for the mechanical stimulation of anterior cruciate ligament grafts. *Biomed Mater Eng*. 2013;23(3): 225-237.
17. Horan RL, Collette AL, Lee C, Antle K, Chen J, Altman GH. Yarn design for functional tissue engineering. *J Biomech*. 2006;39(12): 2232-2240.
18. Horan RL, Toponarski I, Boepple HE, Weitzel PP, Richmond JC, Altman GH. Design and characterization of a scaffold for anterior cruciate ligament engineering. *J Knee Surg*. 2009;22(1):82-92.
19. Hunt P, Scheffler SU, Unterhauser FN, Weiler A. A model of soft-tissue graft anterior cruciate ligament reconstruction in sheep. *Arch Orthop Trauma Surg*. 2005;125(4):238-248.
20. Jang K-M, Lim HC, Jung WY, Moon SW, Wang JH. Efficacy and safety of human umbilical cord blood–derived mesenchymal stem cells in anterior cruciate ligament reconstruction of a rabbit model: new strategy to enhance tendon graft healing. *Arthroscopy*. 2015;31(8):1530-1539.
21. Ju YJ, Muneta T, Yoshimura H, Koga H, Sekiya I. Synovial mesenchymal stem cells accelerate early remodeling of tendon-bone healing. *Cell Tissue Res*. 2008;332(3):469-478.
22. Jurgens WJ, Kroeze RJ, Bank RA, Ritt MJPF, Helder MN. Rapid attachment of adipose stromal cells on resorbable polymeric scaffolds facilitates the one-step surgical procedure for cartilage and bone tissue engineering purposes. *J Orthop Res*. 2011;29(6):853-860.
23. Jurgens WJ, van Dijk A, Doulabi BZ, et al. Freshly isolated stromal cells from the infrapatellar fat pad are suitable for a one-step surgical procedure to regenerate cartilage tissue. *Cytotherapy*. 2009;11(8): 1052-1064.
24. Kaeding CC, Aros B, Pedroza A, et al. Allograft versus autograft anterior cruciate ligament reconstruction: predictors of failure from a MOON prospective longitudinal cohort. *Sports Health*. 2011;3(1):73-81.
25. Kondo E, Yasuda K, Katsura T, Hayashi R, Azuma C, Tohyama H. Local administration of autologous synovium-derived cells improve the structural properties of anterior cruciate ligament autograft reconstruction in sheep. *Am J Sports Med*. 2011;39(5):999-1007.
26. Kondo E, Yasuda K, Yamanaka M, Minami A, Tohyama H. Effects of administration of exogenous growth factors on biomechanical properties of the elongation-type anterior cruciate ligament injury with partial laceration. *Am J Sports Med*. 2005;33(2):188-196.
27. Laitinen O, Pohjonen T, Törmälä P, et al. Mechanical properties of biodegradable poly-L-lactide ligament augmentation device in experimental anterior cruciate ligament reconstruction. *Arch Orthop Trauma Surg*. 1993;112(6):270-274.
28. Leong NL, Arshi A, Kabir N, et al. In vitro and in vivo evaluation of heparin mediated growth factor release from tissue-engineered constructs for anterior cruciate ligament reconstruction. *J Orthop Res*. 2015;33(2):229-236.
29. Leong NL, Petrigliano FA, McAllister DR. Current tissue engineering strategies in anterior cruciate ligament reconstruction. *J Biomed Mater Res A*. 2014;102(5):1614-1624.

30. Li F, Jia H, Yu C. ACL reconstruction in a rabbit model using irradiated Achilles allograft seeded with mesenchymal stem cells or PDGF-B gene-transfected mesenchymal stem cells. *Knee Surg Sports Traumatol Arthrosc*. 2007;15(10):1219-1227.
31. Longo UG, Rizzello G, Berton A, et al. Synthetic grafts for anterior cruciate ligament reconstruction. *Curr Stem Cell Res Ther*. 2013;8(6):429-437.
32. Ma J, Smietana MJ, Kostrominova TY, Wojtys EM, Larkin LM, Arruda EM. Three-dimensional engineered bone–ligament–bone constructs for anterior cruciate ligament replacement. *Tissue Eng Part A*. 2012;18(1-2):103-116.
33. Mayr HO, Stoehr A, Dietrich M, et al. Graft-dependent differences in the ligamentization process of anterior cruciate ligament grafts in a sheep trial. *Knee Surg Sports Traumatol Arthrosc*. 2012;20(5): 947-956.
34. Murray MM, Fleming BC. Use of a bioactive scaffold to stimulate anterior cruciate ligament healing also minimizes posttraumatic osteoarthritis after surgery. *Am J Sports Med*. 2013;41(8):1762-1770.
35. Nau T, Teuschl AH. Regeneration of the anterior cruciate ligament: current strategies in tissue engineering. *World J Orthop*. 2015; 6(1):127.
36. Panas-Perez E, Gatt CJ, Dunn MG. Development of a silk and collagen fiber scaffold for anterior cruciate ligament reconstruction. *J Mater Sci Mater Med*. 2013;24(1):257-265.
37. Petrigliano FA, Arom GA, Nazemi AN, Yeranosian MG, Wu BM, McAllister DR. In vivo evaluation of electrospun polycaprolactone graft for anterior cruciate ligament engineering. *Tissue Eng Part A*. 2015;21(7-8):1228-1236.
38. Proffen BL, McElfresh M, Fleming BC, Murray MM. A comparative anatomical study of the human knee and six animal species. *Knee*. 2013;19(4):493-499.
39. Rathbone S, Maffulli N, Cartmell SH. Most British surgeons would consider using a tissue-engineered anterior cruciate ligament: a questionnaire study. *Stem Cells Int*. 2012;2012:303724.
40. Robertson A, Nutton RW, Keating JF. Current trends in the use of tendon allografts in orthopaedic surgery. *J Bone Joint Surg Br*. 2006;88(8):988-992.
41. Rockwood DN, Preda RC, Yücel T, Wang X, Lovett ML, Kaplan DL. Materials fabrication from Bombyx mori silk fibroin. *Nat Protoc*. 2011;6(10):1612-1631.
42. Serica Technologies Inc. SeriACL™ device (gen IB) trial for anterior cruciate ligament (ACL) repair. NCT00775892. 2008. Available at: http://clinicaltrials.gov/show/NCT00775892. Accessed April 12, 2014.
43. Steadman JR, Cameron-Donaldson ML, Briggs KK, Rodkey WG. A minimally invasive technique (''healing response'') to treat proximal ACL injuries in skeletally immature athletes. *J Knee Surg*. 2006;19(1):8-13.
44. Teuschl AH, van Griensven M, Redl H. Sericin removal from raw bombyx mori silk scaffolds of high hierarchical order. *Tissue Eng Part C Methods*. 2014;20(5):431-439.
45. Van Eijk F, Saris DBF, Riesle J, et al. Tissue engineering of ligaments: a comparison of bone marrow stromal cells, anterior cruciate ligament, and skin fibroblasts as cell source. *Tissue Eng*. 2004;10(5-6):893-903.
46. von Porat A, Roos EM, Roos H. High prevalence of osteoarthritis 14 years after an anterior cruciate ligament tear in male soccer players: a study of radiographic and patient relevant outcomes. *Ann Rheum Dis*. 2004;63(3):269-273.
47. Weiler A, Peine R, Pashmineh-Azar A, Abel C, Südkamp NP, Hoffmann RFG. Tendon healing in a bone tunnel, part I: biomechanical results after biodegradable interference fit fixation in a model of anterior cruciate ligament reconstruction in sheep. *Arthroscopy*. 2002;18(2):113-123.